Journal of Computational Physics **163,** 328–348 (2000)
doi:10.1006/jcph.2000.6562, available online at http://www.idealibrary.com on IDEAL®

A New Method for Solving an Eigenvalue Problem for a System of Three Coulomb Particles within the Hyperspherical Adiabatic Representation

A. G. Abrashkevich,* M. S. Kaschiev,† and S. I. Vinitsky‡

*Chemical Physics Theory Group, Department of Chemistry, University of Toronto, Toronto, Ontario M5S 3H6, Canada; †Institute of Mathematics and Informatics, Bulgarian Academy of Science, Sofia 1113, Bulgaria; and ‡Bogoliubov Laboratory of Theoretical Physics, Joint Institute for Nuclear Research, 141980 Dubna, Moscow Region, Russia
E-mail: aabrash@tikva.chem.utoronto.ca, kaschiev@math.bas.bg, vinitsky@thsun1.jinr.dubna.su

Received October 20, 1999; revised June 15, 2000

The quantum mechanical three-body problem with Coulomb interaction is formulated within the adiabatic representation method using the hyperspherical coordinates. The Kantorovich method of reducing the multidimensional problem to the one-dimensional one is used. A new method for computing variable coefficients (potential matrix elements of radial coupling) of a resulting system of ordinary second-order differential equations is proposed. It allows the calculation of the coefficients with the same precision as the adiabatic functions obtained as solutions of an auxiliary parametric eigenvalue problem. In the method proposed, a new boundary parametric problem with respect to unknown derivatives of eigensolutions in the adiabatic variable (hyperradius) is formulated. An efficient, fast, and stable algorithm for solving the boundary problem with the same accuracy for the adiabatic eigenfunctions and their derivatives is proposed. The method developed is tested on a parametric eigenvalue problem for a hydrogen atom on a three-dimensional sphere that has an analytical solution. The accuracy, efficiency, and robustness of the algorithm are studied in detail. The method is also applied to the computation of the ground-state energy of the helium atom and negative hydrogen ion.

Key Words: three-body problem; Coulomb particles; adiabatic representation; eigenvalue problem; hyperspherical coordinates; boundary parametric problem; potential curves; ground-state energy; helium atom; negative hydrogen ion.

1. INTRODUCTION

During the last few decades, excitation and ionization processes in a system of three charged particles have been actively studied in atomic and molecular physics [1, 2].

0021-9991/00 $35.00

Currently, ongoing work is being carried out at the CERN in the experiments ASACUSA and ATHENA studying properties of exotic antiprotonic Coulomb systems in traps at low temperatures using new abilities of modern lasers [3, 4]. These experiments require various data on characteristics of the Coulomb systems, such as the helium atom He and the antiprotonic helium atom $\bar{p}\mathrm{He}^+$, and also on collision processes, leading to the formation of antiprotonic $\bar{p}\mathrm{He}^{2+}$ and antihydrogen $\bar{\mathrm{H}}$ atoms. Detailed calculations of energy levels and widths of metastable states, radiative and Auger transition rates, collision cross sections, etc., are necessary for the planning and interpretation of the above experiments. Hence, the development of appropriate numerical methods for computing the desired spectroscopic and collision data with sufficient accuracy is an important step in better understanding elementary processes taking place in exotic as well as in regular atomic and molecular systems of charged particles.

One of the most popular and widely used approaches to solving the quantum mechanical three-body problem with Coulomb interaction is the adiabatic representation method [1, 2, 5]. In the framework of the hyperspherical coordinates formulation of this method [2, 6, 7], the hyperradius $\mathcal{R}$ is treated as a slowly varying adiabatic variable, analogous to the internuclear distance in the Born–Oppenheimer approximation for molecules [1]. From a mathematical point of view, this approach is well known as the Kantorovich method for the reduction of a multidimensional boundary problem to the one-dimensional one by using a set of solutions of an auxiliary parametric eigenvalue problem [8]. These solutions are obtained for a given set of values of the adiabatic variable, which plays the role of an external parameter here. The convergence of the adiabatic expansion in the hyperspherical coordinates is faster [9] than the convergence in most conventional approaches based on the independent electron model. This is due to the fact that collective variables such as hyperradius $\mathcal{R} = \sqrt{r_1^2 + r_2^2}$ and hyperangle $\alpha = \tan^{-1}(r_2/r_1)$ allow more natural and accurate accounting for electron correlations in an atomic system (see, e.g., [6]) than the independent electron coordinates, r_1 and r_2.

This method has been successfully applied in calculating energy levels and wave functions of two-electron atoms within the adiabatic hyperspherical approach (see, e.g., [6, 9]), as well as in computing energy spectra of the negative positronium ion Ps^- [7, 10] and various muonic molecules [7, 11] (see also [5, 12]). An essential part of the implementation of the Kantorovich method is the computation of variable coefficients (potential matrix elements) for the final system of ordinary second-order differential equations. These coefficients are the integrals over eigenfunctions and their derivatives with respect to the adiabatic variable. In real applications, efficient and stable computation of derivatives of the adiabatic eigenfunctions and the corresponding integrals with accuracy comparable with that achieved for adiabatic eigenfunctions presents a serious challenge for most of the numerical approaches involved in various types of calculations within the adiabatic representation method.

In the present paper we propose a new numerical method for computing these derivatives with the same accuracy as obtained for the eigenvalues and eigenfunctions of the parametric eigenvalue problem. This circumstance guarantees the calculation of the variable coefficients (potential matrix elements of radial coupling) of a system of ordinary differential equations with the same precision as adiabatic eigenfunctions. This goal is achieved by formulating a new boundary parametric problem with respect to unknown derivatives of eigenvalues and eigenfunctions in the adiabatic variable. An efficient, fast, and stable algorithm for solving this boundary problem with the same precision for the adiabatic eigenfunctions and their derivatives is elaborated.

The accuracy and stability of the method developed are studied on a test parametric problem describing a hydrogen atom on a three-dimensional sphere. This problem has an analytical solution that allows direct comparison of approximate eigensolutions with the exact ones. To show the efficiency and reliability of our implementation of the Kantorovich method, we apply it to the calculation of the ground state energy of the helium atom and negative hydrogen ion. This is a popular problem for three-body Coulomb systems which usually serves as a benchmark for new numerical algorithm and methods. For simplicity, in this paper we consider a system with total angular momentum $J = 0$. This allows us to demonstrate all essential numerical peculiarities of our method when it is applied to a rather complex atomic system without unnecessary complications connected with accounting for additional angular variables for $J > 0$. The generalization of the present approach to three-body systems with arbitrary total angular momentum is straightforward and will be considered elsewhere.

Potential matrix elements of radial coupling obtained within the present approach can be used in scattering calculations using some appropriate propagation scheme (see, e.g., [13]). In scattering calculations, in order to eliminate derivatives of the adiabatic surface eigenfunctions in hyperradius, the sector diabatic approach [14] is widely used. The price for using this approximation is a slower convergence of the diabatic basis and, therefore, there are a larger number of hyperradial equations to be solved to obtain the required accuracy of the S-matrix elements. Matrix elements computed by the present method can be directly incorporated in the popular hyperspherical close-coupling scheme [15]. Applications of the method to scattering problems will be considered elsewhere.

The paper is organized as follows. The Schrödinger equation for a three-dimensional eigenvalue problem for a system of three charged particles is considered in Section 2. The Kantorovich method is briefly described in Section 3. Three steps of implementation of the Kantorovich method are considered in Sections 4–6. In Section 7 our method is applied to three eigenvalue problems. A numerical solution of a parametric eigenvalue problem for a hydrogen atom on a three-dimensional sphere is presented in subsection 7.1. The results of our calculations of the ground-state energy of the helium atom and negative hydrogen ion are presented in Section 7.2, where they are compared to the results of other theretical calculations. The conclusions and possible future developments of the method are discussed in Section 8.

2. THE SCHRÖDINGER EQUATION

A time-independent Schrödinger equation for a system of three charged particles with total angular momentum $J = 0$ in the conventional hyperspherical coordinates $\{\mathcal{R}, \alpha, \theta\}$ [16] can be written as an eigenvalue problem for the following 3-D elliptic equation,

$$\hat{T}\Psi(\mathcal{R}, \alpha, \theta) + \frac{1}{\mathcal{R}}\hat{W}(\alpha, \theta)\Psi(\mathcal{R}, \alpha, \theta) = \mathcal{E}\Psi(\mathcal{R}, \alpha, \theta), \tag{1}$$

where $\mathcal{E}$ is the energy and $\Psi(\mathcal{R}, \alpha, \theta)$ is the total wave function of the system. The differential operator $\hat{T}$ and the Coulomb potential V are defined in Eq. (1) as follows ($e = \hbar = m_e = 1$):

$$\hat{T} = -\frac{1}{\mathcal{R}^2\tau}\frac{\partial}{\partial\mathcal{R}}\frac{1}{2}\mathcal{R}^2\tau\frac{\partial}{\partial\mathcal{R}} + \hat{t},$$

$$\hat{t} = -\frac{1}{\tau}\left(\frac{\partial}{\partial\alpha}\frac{1}{4}\mathcal{R}\sin^2\alpha\sin\theta\frac{\partial}{\partial\alpha} + \frac{\partial}{\partial\theta}\frac{1}{4}\mathcal{R}\sin\theta\frac{\partial}{\partial\theta}\right),$$

$$\hat{W} = \frac{Z_a Z_c}{\sin\alpha/2} + \frac{Z_b Z_c}{\cos\alpha/2} + Z_a Z_b[1 - \sin\alpha\cos\theta]^{-1/2},$$

$$\tau = \frac{1}{8}\mathcal{R}^3 \sin^2\alpha \sin\theta.$$

In the above, $Z_a = Z_b = -1$ and $Z_c = Z$ are the charges of particles a, b, and c with masses $M_a = 1$, $M_b = 1$, and $M_c = \infty$, respectively. Note that $Z = 1$ for the H^- negative hydrogen ion and $Z = 2$ for the He atom. Hyperradius $\mathcal{R} \in [0, \infty)$ and hyperspherical angles $(\alpha, \theta) \in \Omega = \{0 \le \alpha \le \pi, 0 \le \theta \le \pi\}$; i.e., the total set of variables $(\mathcal{R}, \alpha, \theta) \in \Omega_1 = \Omega \times [0, \infty)$.

Total wave function $\Psi(\mathcal{R}, \alpha, \theta)$ satisfies the boundary conditions

$$\lim_{\alpha\to 0,\pi} \sin^2\alpha \frac{\partial\Psi}{\partial\alpha} = 0, \quad \lim_{\theta\to 0,\pi} \sin\theta \frac{\partial\Psi}{\partial\theta} = 0, \tag{2}$$

$$\lim_{\mathcal{R}\to 0} \mathcal{R}^5 \frac{\partial\Psi}{\partial\mathcal{R}} = 0, \quad \lim_{\mathcal{R}\to\infty} \mathcal{R}^5\Psi = 0 \tag{3}$$

and is normalized by the condition

$$\int\int\int \mathcal{R}^2 \tau \Psi^2 \, d\alpha \, d\theta \, d\mathcal{R} = 1.$$

3. KANTOROVICH METHOD

Consider a formal expansion of the solution of Eqs. (1)–(3) over an infinite set of two-dimensional basis functions $\{\Phi_i(\alpha, \theta; \mathcal{R})\}_{i=1}^{\infty}$:

$$\Psi(\mathcal{R}, \alpha, \theta) = \sum_{i=1}^{\infty} \chi_i(\mathcal{R}) \Phi_i(\alpha, \theta; \mathcal{R}). \tag{4}$$

In Eq. (4) the functions $\chi(\mathcal{R})^T = (\chi_1(\mathcal{R}), \chi_2(\mathcal{R}), \ldots)$ are unknown, and the adiabatic functions $\Phi(\alpha, \theta; \mathcal{R})^T = (\Phi_1(\alpha, \theta; \mathcal{R}), \Phi_2(\alpha, \theta; \mathcal{R}), \ldots)$ form an orthonormal basis for each value of the hyperradius $\mathcal{R}$, which is treated here as a slowly varying adiabatic parameter.

In the Kantorovich approach [8], functions $\Phi_i(\alpha, \theta; \mathcal{R})$ are determined as solutions of the two-dimensional eigenvalue problem

$$\left(\hat{t} + \frac{1}{\mathcal{R}}\hat{W}\right)\Phi(\alpha, \theta; \mathcal{R}) = \hat{E}(\mathcal{R})\Phi(\alpha, \theta; \mathcal{R}), \tag{5}$$

with boundary conditions derived from Eq. (2):

$$\lim_{\alpha\to 0,\pi} \sin^2\alpha \frac{\partial\Phi}{\partial\alpha} = 0, \quad \lim_{\theta\to 0,\pi} \sin\theta \frac{\partial\Phi}{\partial\theta} = 0.$$

Since the operator in the left side of Eq. (5) is self-adjoint, its eigenfunctions are orthonormal:

$$\int\int \tau \Phi_i \Phi_j \, d\alpha \, d\theta = \delta_{ij}.$$

In the equation above, δ_{ij} is Kroneker's δ-symbol. Problem (5) is solved for each value of $\mathcal{R}_k \in \omega_{\mathcal{R}}$, where $\omega_{\mathcal{R}} = (\mathcal{R}_1, \mathcal{R}_2, \ldots, \mathcal{R}_k, \ldots)$ is a given set of values of hyperradius $\mathcal{R}$.

After substitution of expansion (4) in the Rayleigh–Ritz variational functional (see [7])

$$R(\Psi) = \int_{\Omega_1} \mathcal{R}^2 \left\{ \frac{1}{2}\tau \left(\frac{\partial \Psi}{\partial \mathcal{R}}\right)^2 + \frac{\mathcal{R}}{4}\sin\theta \left[\sin^2\alpha \left(\frac{\partial \Psi}{\partial \alpha}\right)^2 + \left(\frac{\partial \Psi}{\partial \theta}\right)^2 \right] + \frac{\tau}{\mathcal{R}} \Psi^T \hat{W} \Psi \right\} d\theta\, d\alpha\, d\mathcal{R} \times \left\{ \int_{\Omega_1} \mathcal{R}^2 \Psi^2 \tau\, d\theta\, d\alpha\, d\mathcal{R} \right\}^{-1}$$

and subsequent minimization of the functional, the solution of Eqs. (1)–(3) is reduced to a solution of an eigenvalue problem for an infinite set of ordinary second-order differential equations for determining energy $\mathcal{E}$ and coefficients (radial wave functions) $\chi(\mathcal{R})^T = (\chi_1(\mathcal{R}), \chi_2(\mathcal{R}), \ldots)$ of expansion (4):

$$-\mathbf{I}\frac{1}{\mathcal{R}^2}\frac{d}{d\mathcal{R}}\mathcal{R}^2\frac{d}{d\mathcal{R}}\chi + \mathbf{V}(\mathcal{R})\chi + \mathbf{Q}(\mathcal{R})\frac{d\chi}{d\mathcal{R}} + \frac{1}{\mathcal{R}^2}\frac{d\mathcal{R}^2\mathbf{Q}(\mathcal{R})\chi}{d\mathcal{R}} = 2\mathcal{E}\mathbf{I}\chi, \tag{6}$$

$$\lim_{\mathcal{R}\to 0} \mathcal{R}^2 \frac{\partial \chi}{\partial \mathcal{R}} = 0, \quad \lim_{\mathcal{R}\to\infty} \mathcal{R}^2 \chi = 0. \tag{7}$$

Here $\mathbf{I}$, $\mathbf{V}(\mathcal{R})$, and $\mathbf{Q}(\mathcal{R})$ are infinite matrices, elements of which are given by relations

$$\begin{aligned} I_{ij} &= \delta_{ij}, \quad U_i(\mathcal{R}) = 2E_i(\mathcal{R}) = 2\left(\hat{E}_i(\mathcal{R}) + \frac{2}{\mathcal{R}^2}\right), \\ V_{ij}(\mathcal{R}) &= U_i(\mathcal{R})\delta_{ij} - \frac{1}{4\mathcal{R}^2}\delta_{ij} + H_{ij}(\mathcal{R}), \\ H_{ij}(\mathcal{R}) &= H_{ji}(\mathcal{R}) = \int\int \tau \frac{\partial \Phi_i}{\partial \mathcal{R}} \frac{\partial \Phi_j}{\partial \mathcal{R}}\, d\alpha\, d\theta - \frac{9}{4\mathcal{R}^2}\delta_{ij}, \\ Q_{ij}(\mathcal{R}) &= -Q_{ji}(\mathcal{R}) = \int\int \tau \Phi_i \frac{\partial \Phi_j}{\partial \mathcal{R}}\, d\alpha\, d\theta - \frac{3}{2\mathcal{R}}\delta_{ij}, \quad i, j = 1, 2, \ldots. \end{aligned} \tag{8}$$

Thus, the solution of Sturm–Liouville problem (1)–(3) is reduced to solution of the following three problems:

1. Calculation of potential curves $E_i(\mathcal{R})$ and eigenfunctions $\Phi_i(\alpha, \theta; \mathcal{R})$ of the two-dimensional problem (2)–(5) for a given set of $\mathcal{R} \in \omega_{\mathcal{R}}$.
2. Computation of matrix elements of radial coupling (8) necessary for Eq. (6).
3. Calculation of energies $\mathcal{E}$ and radial wave functions $\chi(\mathcal{R})$ as eigensolutions of one-dimensional eigenvalue problem (6)–(7).

4. SOLUTION OF EIGENVALUE PROBLEM (5)

The two-dimensional parametric eigenvalue problem (2)–(5) can be solved directly [7] using the finite element method [17, 18]. In this paper, we propose a more efficient method of solving this problem. Because of the symmetry of equation coefficients with respect to $\alpha = \pi/2$, problem (5) will be considered for $\alpha \in [0, \pi/2]$.

Consider the expansion of the adiabatic surface function $\Phi_i(\alpha, \theta; \mathcal{R})$

$$\Phi_i(\alpha, \theta; \mathcal{R}) = \sum_{l=0}^{\infty} \varphi_l^{(i)}(\alpha; \mathcal{R}) P_l(\cos\theta), \tag{9}$$

where $\varphi_l^{(i)}(\alpha; \mathcal{R})$ are expansion coefficients depending parametrically on $\mathcal{R}$ and $P_l(\cos\theta)$ are the Legendre polynomials. These polynomials are the eigensolutions of the eigenvalue problem

$$-\frac{d}{d\theta}\sin\theta\frac{dP_l(\cos\theta)}{d\theta} = \lambda\sin\theta P_l(\cos\theta)$$

with $\lambda_l = l(l+1)$ being the corresponding eigenvalues. The Rayleigh–Ritz variational functional for problem (5) can be written as

$$R(\Phi) = \int_0^{\pi/2}\int_0^{\pi}\left[\frac{\mathcal{R}}{4}\sin^2\alpha\sin\theta\left(\frac{\partial\Phi}{\partial\alpha}\right)^2 + \frac{\mathcal{R}}{4}\sin\theta\left(\frac{\partial\Phi}{\partial\theta}\right)^2 + \frac{\mathcal{R}^2}{8}\sin^2\alpha\sin\theta\hat{W}\Phi^2\right]d\theta\,d\alpha \times \left[\int_0^{\pi/2}\int_0^{\pi}\frac{\mathcal{R}^3}{8}\sin^2\alpha\sin\theta\Phi^2\,d\theta\,\alpha\right]^{-1}. \tag{10}$$

Expansion (9) is substituted next into functional (10). After minimization of the variational functional, we see that eigenfunctions $\varphi_l^{(i)}(\alpha; \mathcal{R})$ and eigenvalues $E_i(\mathcal{R})$ satisfy the following eigenvalue problem for an infinite set of ordinary differential equations:

$$L(\varphi, E) \equiv \left[\mathcal{R}\left(-\frac{d}{d\alpha}\mathbf{D}\frac{d}{d\alpha} + \mathbf{\Lambda}\right) + \mathcal{R}^2\mathbf{W} - E_i(\mathcal{R})\frac{1}{2}\mathcal{R}^3\mathbf{D}\right]\varphi = 0, \quad \lim_{\alpha\to 0,\pi/2}\sin^2\alpha\frac{\partial\varphi}{\partial\alpha} = 0. \tag{11}$$

In the above, $\mathbf{D}$, $\mathbf{\Lambda}$, and $\mathbf{W}$ are infinite matrices, elements of which are defined by

$$D_{ii} = \frac{1}{4}\sin^2\alpha, \quad D_{ij} = 0, \quad i \neq j, \quad \Lambda_{ii} = \frac{1}{4}(i(i+1) + \sin^2\alpha), \quad \Lambda_{ij} = 0, \quad i \neq j,$$

$$W_{ij} = -Z\frac{1}{4}\sin\alpha\left(\cos\frac{\alpha}{2} + \sin\frac{\alpha}{2}\right)\delta_{ij} + \frac{1}{8}\sin^2\alpha W_{ij}^{\text{rep}},$$

$$W_{ij}^{\text{rep}} = \int_{-1}^{1}\frac{P_i(t)P_j(t)}{\sqrt{1 - t\sin\alpha}}\,dt, \quad i, j = 0, 1, 2, \ldots.$$

Thus, the solution of the two-dimensional eigenvalue problem (2)–(5) is reduced to the solution of eigenvalue problem (11) for a system of the ordinary second-order differential equations. Note that in Eq. (11) instead of eigenvalues $\hat{E}_i(\mathcal{R})$ we have used shifted eigenvalues $E_i(\mathcal{R}) = \hat{E}_i(\mathcal{R}) + 2/\mathcal{R}^2$ which are obtained as solutions of Eq. (5) by adding the extra term $2/\mathcal{R}^2$ to the adiabatic Hamiltonian. $E_i(\mathcal{R})$ were introduced earlier in definition (8) and correspond to eigenvalues of the conventional parametric eigenvalue problem [24].

5. SOLUTION OF EIGENVALUE PROBLEMS (6) AND (11)

For a numerical solution of one-dimensional eigenvalue problems (6) and (11) subject to the corresponding boundary conditions, the high-order approximations of the finite-element method [17, 18] elaborated in our previous papers [19, 20] have been used. One-dimensional finite elements of order $p = 1, 2, \ldots, 10$ have been implemented. Using the standard finite-element procedures [18], problems (6) and (11) are approximated by the generalized algebraic eigenvalue problem

$$\mathbf{A}\mathbf{F}^h = E^h\mathbf{B}\mathbf{F}^h, \tag{12}$$

where $\mathbf{A}$ is the stiffness matrix, $\mathbf{B}$ is the mass matrix, E^h is the corresponding eigenvalue, and $\mathbf{F}^h$ is the vector approximating solutions of (6) or (11) on the finite-element grid. For problem (6), $\mathbf{A} = \tilde{\mathbf{K}}_1 + \tilde{\mathbf{K}}_2 + \tilde{\mathbf{K}}_3$ and $\mathbf{B} = \tilde{\mathbf{M}}$, where matrices $\tilde{\mathbf{K}}_1$, $\tilde{\mathbf{K}}_2$, and $\tilde{\mathbf{K}}_3$ correspond to the first, the second, and the third and fourth terms on the left-hand side of Eq. (6), respectively, and matrix $\tilde{\mathbf{M}}$ corresponds to the term on the right-hand side of Eq. (6). For problem (11), $\mathbf{A} = \mathcal{R}\mathbf{K}_1 + \mathcal{R}^2\mathbf{K}_2$ and $\mathbf{B} = \mathcal{R}^3\mathbf{M}$, where matrices $\mathbf{K}_1$, $\mathbf{K}_2$, and $\mathbf{M}$ correspond to the first, the second, and the third terms in Eq. (11), respectively. The $\mathbf{A}$ and $\mathbf{B}$ matrices are symmetric and have a banded structure, and the $\mathbf{B}$ matrix is also positive definite. The algebraic eigenvalue problem (12) is solved using the subspace iteration method [18].

Let E_n, φ_n be the exact solution of (11) and let $E_n^h, \mathbf{F}_n^h$ be the numerical solution of (12). Then the following estimates are valid [17],

$$\left|E_n - E_n^h\right| \le c_1(E_n)h^{2p}, \quad \left\|\varphi_n - \mathbf{F}_n^h\right\|_0 \le c_2(E_n)h^{p+1}, \qquad c_1 > 0, \quad c_2 > 0, \tag{13}$$

where h is the grid step, p is the order of finite elements, n is the number of the corresponding eigensolution, and constants c_1 and c_2 do not depend on step h. The same estimates are valid for the approximate solutions of problem (6).

6. CALCULATIONS OF MATRIX ELEMENTS OF RADIAL COUPLING

Calculation of the potential matrices $\mathbf{V}(\mathcal{R})$ and $\mathbf{Q}(\mathcal{R})$ (see Eq. (8)) with sufficiently high accuracy is a very important step in solving a system of radial equations (6); otherwise, it is practically impossible to get the desired energies and wave functions of three-body Coulomb systems with the required precision. This implies that derivatives $\frac{d\varphi}{d\mathcal{R}}$ should be computed with the highest possible accuracy, which presents a difficult problem for most of the numerical methods usually used in the adiabatic representation calculations. In most applications the formulas

$$Q_{ij}(\mathcal{R}) = [\mathcal{R}(E_i(\mathcal{R}) - E_j(\mathcal{R}))]^{-1} \int_0^{\pi/2} \varphi_i^T \mathcal{R}^2 \mathbf{W} \varphi_j \, d\alpha \tag{14}$$

and

$$H_{ij}(\mathcal{R}) = -\sum_l Q_{il}(\mathcal{R}) Q_{lj}(\mathcal{R}), \quad Q_{ii}(\mathcal{R}) = 0 \tag{15}$$

are used. Note that Eq. (15) has rather slow convergence, which means that to obtain a high level of accuracy one should include a sufficiently large number of terms in a sum over l.

This circumstance can present a serious problem from the computational point of view, especially with regard to demands for required computational resources and computation time.

The main goal of this paper is to develop an effective numerical method that will allow one to calculate derivative $\frac{d\varphi}{d\mathcal{R}}$ with the same accuracy as achieved for eigenfunctions of (11) and to use it to compute matrix elements defined by formulas (8). Taking a derivative of (11) with respect to $\mathcal{R}$, we see that $\frac{d\varphi}{d\mathcal{R}}$ can be obtained as a solution of the following boundary problem:

$$L\left(\frac{d\varphi}{d\mathcal{R}}, E\right) = \left[\frac{d}{d\alpha}\mathbf{D}\frac{d}{d\alpha} - \mathbf{\Lambda} - 2\mathcal{R}\mathbf{W} + \frac{3}{2}E(\mathcal{R})\mathcal{R}^2\mathbf{D} + \frac{1}{2}E'(\mathcal{R})\mathcal{R}^3\mathbf{D}\right]\varphi \equiv G. \quad (16)$$

The boundary conditions for function $\frac{d\varphi}{d\mathcal{R}}$ are the same as for function φ. Taking into account that $E(\mathcal{R})$ is an eigenvalue of operator L, problem (16) will have a solution *if and only if the right-hand side term G is orthogonal to the eigenfunction* φ. From this condition we find that

$$E'(\mathcal{R}) = \int_0^{\pi/2}\left[\frac{d\varphi}{d\alpha}^T\mathbf{D}\frac{d\varphi}{d\alpha} + \varphi^T(\mathbf{\Lambda} + 2\mathcal{R}\mathbf{W})\varphi\right]d\alpha - \frac{3}{\mathcal{R}}E(\mathcal{R}). \quad (17)$$

Now the problem (16) has a solution, but it is not unique. From the normalization condition

$$\int_0^{\pi/2}\varphi^T\frac{1}{2}\mathcal{R}^3\mathbf{D}\varphi\, d\alpha = 1$$

we obtain the required additional condition

$$\int_0^{\pi/2}\varphi^T\frac{1}{2}\mathcal{R}^3\mathbf{D}\frac{d\varphi}{d\mathcal{R}}\, d\alpha = -\frac{3}{2\mathcal{R}}. \quad (18)$$

Thus, problem (16) with additional conditions (17)–(18) has now a unique solution. It is necessary to mention that the second estimate of Eq. (13) is valid also for solution $\frac{d\varphi}{d\mathcal{R}}$ of problem (16)–(18). This fact guarantees the same accuracy for adiabatic functions and their derivatives within the present method.

Let us consider a numerical algorithm for the computation of the derivative $\frac{d\varphi}{d\mathcal{R}}$. It follows from Eq. (12) that we should solve the linear system of algebraic equations

$$\mathbf{Ku} \equiv (\mathbf{A} - E^h\mathbf{B})\mathbf{u} = \mathbf{b}, \quad \mathbf{u} = \frac{d\mathbf{F}^h}{d\mathcal{R}}, \quad (19)$$

where

$$\mathbf{A} = \mathcal{R}\mathbf{K}_1 + \mathcal{R}^2\mathbf{K}_2, \quad \mathbf{B} = \mathcal{R}^3\mathbf{M},$$

$$\mathbf{b} = [-\mathbf{K}_1 - 2\mathcal{R}\mathbf{K}_2 + (3E^h + \mathcal{R}(E^h)')\mathcal{R}^2\mathbf{M}]\mathbf{F}^h,$$

$$(E^h)' = (\mathbf{F}^h)^T[\mathbf{K}_1 + 2\mathcal{R}\mathbf{K}_2]\mathbf{F}^h - \frac{3}{\mathcal{R}}E^h.$$

In these expressions $\mathbf{K}_1$, $\mathbf{K}_2$, and $\mathbf{M}$ are the finite-element matrixes which correspond to the first, second, and third terms in Eq. (11) with $\mathcal{R} = 1$. Since E^h is an eigenvalue of (12), matrix $\mathbf{K}$ in Eq. (19) is degenerate. The algorithm for solving Eq. (19) can be written in three steps as follows:

Step 1. The additional condition (18) has the form

$$\mathbf{u}^T \mathbf{B}\mathbf{F}^h = -\frac{3}{2\mathcal{R}}.$$

Denote by k a number determined by the condition

$$|\mathbf{B}\mathbf{F}^h|_k = \max_{1 \le i \le N} |\mathbf{B}\mathbf{F}^h|_i, \quad C_k = (\mathbf{B}\mathbf{F}^h)_k,$$

where N is the order of matrices above.

Step 2. Solve two systems of algebraic equations

$$\bar{\mathbf{K}}\bar{v} = \bar{\mathbf{b}}, \quad \bar{\mathbf{K}}\bar{w} = \mathbf{c},$$

where

$$\mathbf{c}^T = (K_{1k}, K_{2k}, \ldots, K_{Nk}), \quad c_k = 0, \quad \bar{b}_i = b_i, \quad \bar{b}_k = 0,$$
$$\bar{\mathbf{K}}_{ij} = \mathbf{K}_{ij}, \quad i \ne k, \quad j \ne k, \quad \bar{\mathbf{K}}_{ik} = 0, \quad i \ne k, \quad \bar{\mathbf{K}}_{kj} = 0, \quad j \ne k, \quad \bar{\mathbf{K}}_{kk} = 1.$$

In this way we have $\bar{v}_k = 0$ and $\bar{w}_k = 0$.

Step 3. Find constants γ, γ_1, and γ_2 as

$$\gamma_1 = \bar{\mathbf{v}}^T \mathbf{B}\mathbf{F}^h, \quad \gamma_2 = \bar{\mathbf{w}}^T \mathbf{B}\mathbf{F}^h, \quad \gamma = -\frac{3 + 2\mathcal{R}\gamma_1}{2\mathcal{R}(C_k - \gamma_2)}.$$

After this, the derivative $\mathbf{u} = \frac{d\mathbf{F}^h}{d\mathcal{R}}$ is obtained using the formula

$$u_i = \bar{v}_i - \gamma \bar{w}_i, \quad i \ne k, \quad u_k = \gamma.$$

From the considerations above, it is evident that the derivative computed has the same accuracy as the calculated eigenfunction.

7. NUMERICAL RESULTS

In this section we apply our approach to three problems which allow us to demonstrate the high accuracy, efficiency, and stability of the algorithm developed. The first test problem solves the eigenvalue problem for a hydrogen atom on a three-dimensional sphere. This problem has an analytical solution, which allows direct comparison of approximate eigensolutions obtained by our method to the exact solutions. The other two problems are devoted to the computation of the ground-state energy of the helium atom and the negative hydrogen ion, respectively. Such eigenvalue problem is usually used as a benchmark for testing the accuracy of numerical methods for solving three-body Coulomb problems since high precision variational calculations are available for comparison.

7.1. *Hydrogen Atom on a Three-Dimensional Sphere*

Consider the following eigenvalue problem:

$$\left(-\frac{1}{2\sin^2\alpha}\frac{d}{d\alpha}\sin^2\alpha\frac{d}{d\alpha}-\frac{1}{\mathcal{R}}\cot\alpha\right)\psi(\alpha;\mathcal{R})=E(\mathcal{R})\psi(\alpha;\mathcal{R}),$$
$$\lim_{\alpha\to 0}\sin^2\alpha\frac{\partial\psi}{\partial\alpha}=0,\quad \lim_{\alpha\to\pi}\sin^2\alpha\frac{\partial\psi}{\partial\alpha}=0. \tag{20}$$

To preserve the form of the operators used in previous sections, we rewrite Eq. (20) as

$$\left(-\mathcal{R}\frac{d}{d\alpha}\sin^2\alpha\frac{d}{d\alpha}-\mathcal{R}^2\sin 2\alpha\right)\psi(\alpha;\mathcal{R})=E(\mathcal{R})2\mathcal{R}^3\sin^2\alpha\psi(\alpha;\mathcal{R}).$$

Problem (20) has an analytical solution,

$$E_n(\mathcal{R})=-\frac{1}{2}\left[\frac{1}{n^2}-\frac{n^2-1}{\mathcal{R}^2}\right],\quad n=1,2,\ldots,$$

with eigenfunctions $\psi_n(\alpha;\mathcal{R})$ which are the radial functions of a hydrogen atom on a three-dimensional sphere [21, 22],

$$\psi_n(\alpha,\mathcal{R})=C_n(\mathcal{R})\,\mathrm{Re}\{\exp[-\imath\alpha(n-1-\imath\sigma)]_2F_1(-n+1,1+\imath\sigma,2,1-\exp(2\imath\alpha))\},$$
$$C_n(\mathcal{R})=\frac{2}{\sqrt{1-\exp(-2\pi\sigma)}}\sqrt{\sigma\frac{n^2+\sigma^2}{\mathcal{R}^3}},\quad \sigma=\frac{\mathcal{R}}{n},$$

where ${}_2F_1$ is a full hypergeometric function.

Denote the exact solutions of problem (20) by (E_n,ψ_n) and the numerical ones by (E_n^h,ψ_n^h). First, we present the results of the computation of eigenvalues and their derivatives, which were obtained using 100 finite elements of the fifth order (501 nodes). Twenty eigenvalues were calculated simultaneously at two values of hyperradius, $\mathcal{R}=1$ and 15 a.u. Some of them are presented in Tables I and II together with the quantities $\epsilon=E_n^h-E_n$ and $\delta=(E_n^h)'-E_n'$, which show the actual accuracy achieved for the approximate eigenvalues and their derivatives. From the tables, one can see the excellent agreement (10^{-10} or better) of our numerical results with the exact solutions.

In order to compare the accuracy of radial matrix elements computed from the analytical and numerical solutions, we denote matrices $\mathbf{Q}$ and $\mathbf{H}$ calculated using exact solutions (E_n,ψ_n) with the help of expressions (8) and (14)–(15) by $\mathbf{Q}^1$, $\mathbf{H}^1$ and $\mathbf{Q}^2$, $\mathbf{H}^2$, respectively, and the ones calculated from (E_n^h,ψ_n^h) by $\mathbf{Q}^{1\mathrm{h}}$, $\mathbf{H}^{1\mathrm{h}}$ and $\mathbf{Q}^{2\mathrm{h}}$, $\mathbf{H}^{2\mathrm{h}}$, respectively. To simplify the comparison between the analytical and numerical solutions we introduce the following quantities:

$$q_1=\max_{1\le i,j\le 20}\left|Q_{ij}^1-Q_{ij}^{1h}\right|,\quad q_2=\max_{1\le i,j\le 20}\left|Q_{ij}^2-Q_{ij}^{2h}\right|,\quad q_3=\max_{1\le i,j\le 20}\left|Q_{ij}^{1h}-Q_{ij}^{2h}\right|,$$
$$h_1=\max_{1\le i,j\le 20}\left|H_{ij}^1-H_{ij}^{1h}\right|,\quad h_2=\max_{1\le i,j\le 20}\left|H_{ij}^2-H_{ij}^{2h}\right|,\quad h_3=\max_{1\le i,j\le 20}\left|H_{ij}^{1h}-H_{ij}^{2h}\right|.$$

In Table III we compare the results of our computations with the analytical solutions obtained for $\mathcal{R}=1$ and 15 a.u. One can see that radial matrix elements calculated within the present approach agree very well (10^{-8} or better) with the exact ones for the given values of $\mathcal{R}$.

TABLE I

Approximate Eigenvalues E_n^h for a Hydrogen Atom on a Three Dimensional Sphere and Their Derivatives $(E_n^h)'$ Calculated at $\mathcal{R} = 1$ a.u., $\epsilon = E_n^h - E_n$, and $\delta = (E_n^h)' - E_n'$, Where E_n and E_n' Are Exact Solutions

n	E_n^h	ϵ	$(E_n^h)'$	δ
1	−0.4999999999(+00)	0.266(−11)	−0.5748734821(−11)	0.575(−11)
2	0.1375000000(+01)	0.253(−11)	−0.3000000000(+01)	−0.264(−11)
3	0.3944444444(+01)	0.986(−12)	−0.8000000000(+01)	−0.101(−11)
4	0.7468750000(+01)	0.476(−12)	−0.1500000000(+02)	−0.490(−12)
5	0.1198000000(+02)	0.125(−12)	−0.2400000000(+02)	−0.111(−12)
6	0.1748611111(+02)	0.137(−12)	−0.3500000000(+02)	−0.154(−12)
8	0.3149218750(+02)	0.122(−13)	−0.6300000000(+02)	−0.246(−13)
10	0.4949499999(+02)	0.301(−13)	−0.9900000000(+02)	−0.144(−14)
12	0.7149652777(+02)	0.793(−13)	−0.1429999999(+03)	−0.761(−13)
14	0.9749744897(+02)	0.114(−12)	−0.1949999999(+03)	−0.108(−12)
16	0.1274980468(+03)	0.105(−12)	−0.2549999999(+03)	−0.100(−12)
18	0.1614984567(+03)	0.310(−13)	−0.3229999999(+03)	−0.191(−12)
20	0.1994987500(+03)	0.464(−12)	−0.3990000000(+03)	−0.107(−09)

Note. The numbers in parentheses denote a powers of 10.

TABLE II

The Same as in Table I for $\mathcal{R} = 15$ a.u.

n	E_n^h	ϵ	$(E_n^h)'$	δ
1	−0.4999999999(+00)	0.857(−11)	0.6063205493(−12)	0.606(−12)
2	−0.1183333333(+00)	0.353(−11)	−0.8888888888(−03)	−0.600(−10)
3	−0.3777777777(−01)	0.377(−11)	−0.2370370370(−02)	−0.689(−11)
4	0.2083333333(−02)	0.431(−10)	−0.4444444444(−02)	−0.179(−11)
5	0.3333333333(−01)	0.261(−11)	−0.7111111111(−02)	−0.113(−12)
6	0.6388888888(−01)	0.144(−11)	−0.1037037037(−01)	−0.555(−12)
8	0.1321875000(+00)	0.761(−12)	−0.1866666666(−01)	−0.305(−13)
10	0.2150000000(+00)	0.496(−12)	−0.2933333333(−01)	−0.459(−12)
12	0.3143055555(+00)	0.352(−12)	−0.4237037037(−01)	−0.938(−13)
14	0.4307823129(+00)	0.252(−12)	−0.5777777777(−01)	−0.294(−12)
16	0.5647135416(+00)	0.247(−12)	−0.7555555555(−01)	−0.125(−12)
18	0.7162345679(+00)	0.363(−12)	−0.9570370370(−01)	−0.173(−12)
20	0.8854166666(+00)	0.823(−12)	−0.1182222222(+00)	−0.782(−10)

TABLE III

Comparison between Analytical and Numerical Matrix Elements Calculated Using Exact Solutions (E_n, ψ_n) and the Approximate Ones, (E_n^h, ψ_n^h)

$\mathcal{R}$	q_1	q_2	q_3	h_1	h_2
$\mathcal{R} = 1$	0.308(−08)	0.593(−11)	0.732(−11)	0.381(−08)	0.461(−08)
$\mathcal{R} = 15$	0.663(−08)	0.178(−14)	0.696(−13)	0.787(−08)	0.817(−08)

Note. Quantities q_1, q_2, q_3, h_1, and h_2 are defined in the text. The numerical scheme parameters are the same as those in Table I.

TABLE IV
Convergence of the h_3^m as a Function of the Number of Adiabatic Eigensolutions m (m = 5, 10, 15, 20)

$\mathcal{R}$	h_3^5	h_3^{10}	h_3^{15}	h_3^{20}
$\mathcal{R}=1$	0.473(−06)	0.342(−05)	0.133(−04)	0.162(−02)
$\mathcal{R}=15$	0.195(−04)	0.195(−04)	0.195(−04)	0.127(−02)

Note. h_3^m is defined in the text.

Note that our numerical results are also in excellent agreement with theoretical estimates (13).

Consider next the convergence of formula (15) with respect to the size of the adiabatic basis set (number of parametric eigenvalues $E_i(\mathcal{R})$). To do that we have calculated the following constructs:

$$H_{ij}^{2h,m} = -\sum_{l}^{m} Q_{il} Q_{lj}, \quad 1 \le i, j \le m, \quad m = 1, 2, \ldots, 20.$$

The results for the h_3^m calculated from the H_{ij}^{1h} and $H_{ij}^{2h,m}$ for some values of m are shown in Table IV. From the table, we can see that the matrix elements $H_{ij}^{2h,m}$ calculated using formula (15) show poor convergence in m and therefore lower accuracy and computational efficiency in comparison with the ones obtained from Eqs. (8). This result is important in the context of the next section since to obtain the desired level of accuracy of solutions for a three-body problem within the adiabatic representation we need to calculate potential matrices $\mathbf{Q}(\mathcal{R})$ and $\mathbf{U}(\mathcal{R})$ with the same accuracy as surface functions $\Phi_i(\alpha, \theta; \mathcal{R})$. The fulfillment of this requirement is guaranteed in the proposed approach.

7.2. *Helium Atom and Negative Hydrogen Ion*

In this section we present numerical results of solving problem (1)–(3) for the ground state of the helium atom and for the negative hydrogen ion. First, let us examine the accuracy of the potential curves $E_i(\mathcal{R})$ and potential matrix elements $Q_{ij}(\mathcal{R})$ and $H_{ij}(\mathcal{R})$ within the present method for the helium atom. These calculations can be compared directly with the results of calculations for the helium atom performed in Refs. [23, 24] using another implementation of the adiabatic hyperspherical approach. In [23, 24], a different numerical method for constructing the adiabatic functions $\Phi_i(\alpha, \theta; \mathcal{R})$ has been used. Matrix elements $Q_{ij}(\mathcal{R})$ were calculated in [23, 24] as

$$Q_{ij}(\mathcal{R}) = [\mathcal{R}^2(E_i(\mathcal{R}) - E_j(\mathcal{R}))]^{-1} \langle \Phi_i(\alpha, \theta; \mathcal{R}) | \hat{W}(\alpha, \theta) | \Phi_j(\alpha, \theta; \mathcal{R}) \rangle \qquad (21)$$

and $H_{ij}(\mathcal{R})$ were obtained from Eq. (15). To compare our results with the ones reported in [24], we have calculated potential curves $E_i(\mathcal{R})$, $i = 1, \ldots, 6$, and potential matrix elements $Q_{ij}(\mathcal{R})$ and $H_{ij}(\mathcal{R})$, $i, j = 1, \ldots, 6$, at a fixed value of hyperradius $\mathcal{R} = 7.65$ a.u. To solve Eq. (11), consisting of seven equations, ($l_{\max} = 6$), 68 finite elements of the seventh order (477 nodes) have been used. Our results for the E_i ($\mathcal{R} = 7.65$) and Q_{ij}^{1h} ($\mathcal{R} = 7.65$) agree very well with the Q_{ij}^{2h} ($\mathcal{R} = 7.65$) obtained from Eq. (21) in [24] with the same number and

TABLE V

Eigenvalues (Adiabatic Potential Curves) $E_i(\mathcal{R})$ and Their Derivatives $dE_i(\mathcal{R})/d\mathcal{R}$, $i = 1, \ldots, 6$, Computed at $\mathcal{R} = 7.65$ a.u.

i	E_i^h	$\tilde{E}_i^h$	$\bar{E}_i^h$	$(E_i^h)'$
1	−2.13590169	−2.1358893	−2.1358894	0.18574453(−01)
2	−0.698907137	−0.69893960	−0.69893964	0.46093945(−01)
3	−0.617951769	−0.61794757	−0.61794766	0.19973460(−01)
4	−0.422639095	−0.42279391	−0.42279421	−0.22691387(−01)
5	−0.371634497	−0.37170963	−0.37171011	−0.16109094(−01)
6	−0.269808873	−0.26968352	−0.26968483	−0.21915412(−01)

Note. E_i^h, $(E_i^h)'$, $\tilde{E}_i^h$, and $\bar{E}_i^h$ are explained in the text.

order of finite elements (477 grid points), $l_{\max} = 6$, and $k_{\max} = 8$ ($k_{\max}$ here is the number of eigenvalues of the auxiliary one-dimensional adiabatic Hamiltonian [24]). However, some of our matrix elements H_{ij}^{1h} ($\mathcal{R} = 7.65$) differ significantly (up to a factor of 1.7) from the H_{ij}^{2h} ($\mathcal{R} = 7.65$) elements obtained in [24]. Analysis of these results (presented below in Table VII) has showed that to obtain better agreement between the two methods for the $H_{ij}(\mathcal{R})$, it is necessary to increase the value of $k_{\max}$ from 8 to 15 and also to increase the number of terms in sum (15) from 6 to at least 80. Only this significantly extended basis set enables matrix elements H_{ij}^{2h} ($\mathcal{R} = 7.65$) calculated by the method of Ref. [24] to approach those obtained by using Eq. (8).

In Table V we present the results of our calculations of potential curves E_i^h and their derivatives $(E_i^h)'$, $i = 1, \ldots, 6$, calculated with relative error tolerance of 10^{-10} a.u. at $\mathcal{R} = 7.65$ a.u. Seven differential equations (11) ($l_{\max} = 6$) have been solved using 68 finite elements of the seventh order (477 nodes). For comparison, the results of the computations of the $\tilde{E}_i^h$ and $\bar{E}_i^h$ for two different sets of numerical parameters carried out by the method of Ref. [24] are given in the third and fourth columns, respectively. The $\tilde{E}_i^h$ have been computed in [24] using 68 finite elements of the seventh order with $l_{\max} = 6$ and $k_{\max} = 8$. The $\bar{E}_i^h$, $i = 1, \ldots, 80$, have been obtained using the same number and order of finite elements with $l_{\max} = 6$ and $k_{\max} = 15$ (only the first six eigenvalues are displayed). One can see that there is very good agreement between the calculations presented in the table. However, it is important to mention that eigenvalues E_i^h are solutions of Eq. (11) obtained using zero-gradient (Neumann) boundary conditions, whereas $\tilde{E}_i^h$ and $\bar{E}_i^h$ have been obtained as solutions of the auxiliary one-dimensional eigenvalue problem (see Eq. (12) of Ref. [24]) using zero-value (Dirichlet) boundary conditions. Also, matrix elements V_{ij} are calculated using different approaches (compare Eq. (11) of Ref. [24] and Eq. (11) and the formula for V_{ij} below Eq. (11) in the present work), which results in the different rate of convergence of the corresponding angular expansions.

In Table VI we present our calculations of matrix elements Q_{ij}^{1h} ($\mathcal{R} = 7.65$) and Q_{ij}^{2h} ($\mathcal{R} = 7.65$) obtained from formulas (8) and (14), respectively. The results of both calculations are practically identical within the given accuracy. For comparison, we show in Table VI matrix elements $\tilde{Q}_{ij}^{2h}$ ($\mathcal{R} = 7.65$) (the fifth column) obtained by formula (21) in [24] and also $\bar{Q}_{ij}^{2h}$ ($\mathcal{R} = 7.65$) (the sixth column) calculated by the same method but using the extended basis set described above. One can see very good agreement between all four calculations presented in the table.

In Table VII we present our results for radial matrix elements H_{ij}^{1h} ($\mathcal{R} = 7.65$) and H_{ij}^{2h} ($\mathcal{R} = 7.65$) obtained within the present approach using formulas (8) and (15), respectively.

TABLE VI

Matrix Elements of Radial Coupling $Q_{ij}(\mathcal{R})$ Computed at $\mathcal{R}$ = 7.65 a.u.

i	j	Q_{ij}^{1h}	Q_{ij}^{2h}	$\tilde{Q}_{ij}^{2h}$	$\bar{Q}_{ij}^{2h}$
1	2	0.586014(−01)	0.586014(−01)	0.585907(−01)	0.585893(−01)
1	3	−0.286341(−01)	0.286341(−01)	0.286413(−01)	0.286418(−01)
1	4	0.442209(−01)	0.442209(−01)	0.442198(−01)	0.442216(−01)
1	5	−0.336214(−01)	−0.336214(−01)	0.336215(−01)	0.336233(−01)
1	6	0.161869(−01)	0.161869(−01)	0.162012(−01)	0.162002(−01)
2	3	0.250621(−01)	0.250621(−01)	−0.250045(−01)	−0.250077(−01)
2	4	0.165765(+00)	0.165765(+00)	0.165781(+00)	0.165782(+00)
2	5	−0.607837(−01)	−0.607837(−01)	0.607890(−01)	0.607908(−01)
2	6	0.172490(−01)	0.172490(−01)	0.172592(−01)	0.172573(−01)
3	4	0.457925(−01)	0.457925(−01)	−0.458364(−01)	−0.458311(−01)
3	5	0.134640(+00)	0.134640(+00)	0.134615(+00)	0.134617(+00)
3	6	−0.896893(−01)	−0.896893(−01)	0.897034(−01)	0.897034(−01)
4	5	−0.203183(+00)	−0.203183(+00)	0.202920(+00)	0.202961(+00)
4	6	0.155380(−01)	0.155380(−01)	0.155163(−01)	0.155172(−01)
5	6	−0.113957(+00)	−0.113957(+00)	0.113800(+00)	0.113799(+00)

Note. Q_{ij}^{1h}, Q_{ij}^{2h}, $\tilde{Q}_{ij}^{2h}$, and $\bar{Q}_{ij}^{2h}$ are defined in the text.

The results for the H_{ij}^{2h} ($\mathcal{R} = 7.65$) have been obtained using six terms in sum (15). One can easily see a big difference between these two calculations. A similar discrepancy is observed between the H_{ij}^{1h} ($\mathcal{R} = 7.65$) and the $\tilde{H}_{ij}^{2h}$ ($\mathcal{R} = 7.65$) (the fifth column in Table VII) taken from Ref. [24]. As expected, our H_{ij}^{2h} ($\mathcal{R} = 7.65$) elements agree much better with the

TABLE VII

Matrix Elements of Radial Coupling $H_{ij}(\mathcal{R})$ Computed at $\mathcal{R}$ = 7.65 a.u.

i	j	H_{ij}^{1h}	H_{ij}^{2h}	$\tilde{H}_{ij}^{2h}$	$\bar{H}_{ij}^{2h}$
1	1	0.129180(−01)	0.760195(−02)	0.760548(−02)	0.128801(−01)
1	2	0.126385(−01)	0.893549(−02)	0.947869(−02)	0.126303(−01)
1	3	−0.729629(−02)	−0.542228(−02)	0.648605(−02)	0.728683(−02)
1	4	0.376942(−02)	−0.132001(−02)	−0.129332(−02)	0.375300(−02)
1	5	−0.105365(−01)	0.145577(−01)	−0.145408(−01)	−0.105361(−01)
1	6	−0.599567(−02)	−0.809748(−02)	−0.825414(−02)	−0.599308(−02)
2	2	0.387063(−01)	0.355324(−01)	0.372254(−01)	0.387056(−01)
2	3	−0.450057(−02)	−0.381820(−02)	0.593952(−02)	0.449231(−02)
2	4	0.190126(−01)	0.140620(−01)	0.244742(−01)	0.189969(−01)
2	5	0.238220(−01)	0.263704(−01)	−0.156242(−01)	−0.238009(−01)
2	6	−0.538306(−02)	−0.630598(−02)	−0.799195(−02)	−0.537534(−02)
3	3	0.326976(−01)	0.297171(−01)	0.731349(−01)	0.326953(−01)
3	4	−0.256900(−01)	−0.258621(−01)	0.251212(−02)	0.256612(−01)
3	5	0.226722(−01)	0.189643(−01)	−0.677882(−02)	0.226588(−01)
3	6	0.119753(−01)	0.146004(−01)	−0.185494(−01)	−0.119490(−01)
4	4	0.814621(−01)	0.730553(−01)	−0.374142(+00)	0.813717(−01)
4	5	−0.966072(−02)	−0.716772(−02)	−0.307431(+00)	0.965263(−02)
4	6	−0.23124(−01)	−0.236861(−01)	0.370903(+00)	−0.230691(−01)
5	5	0.834146(−01)	0.772227(−01)	0.264643(+00)	0.832770(−01)
5	6	−0.194731(−01)	−0.168255(−01)	0.402133(−01)	0.194682(−01)
6	6	0.273542(−01)	0.218313(−01)	−0.499955(−02)	0.273217(−01)

Note. H_{ij}^{1h}, H_{ij}^{2h}, $\tilde{H}_{ij}^{2h}$, and $\bar{H}_{ij}^{2h}$ are defined in the text.

$\tilde{H}_{ij}^{2h}$ ($\mathcal{R} = 7.65$) obtained with the same number of terms in formula (15). Such disagreement between the H_{ij}^{1h} and the H_{ij}^{2h} and $\tilde{H}_{ij}^{2h}$ is because of the insufficient number of terms (six only) taken into account in sum (15) for the H_{ij}^{2h} and $\tilde{H}_{ij}^{2h}$. In order to show that matrix elements H_{ij}^{1h} are much more accurate than the H_{ij}^{2h} and $\tilde{H}_{ij}^{2h}$ ones, we have calculated the $\bar{H}_{ij}^{2h}$ (see the sixth column in Table VII) using 80 terms in sum (15). Comparison of the third and sixth columns in Table VII clearly indicates that the $\bar{H}_{ij}^{2h}$ computed with the extended basis set parameters agree much better with the H_{ij}^{1h} obtained by Eq. (8) than with the H_{ij}^{2h} and $\tilde{H}_{ij}^{2h}$ computed by Eq. (15). This confirms our conclusion about the higher accuracy and efficiency of formulas (8) and the necessity to use a rather large number of terms in Eq. (15) (and therefore excessive computational resources) to obtain comparable accuracy of matrix elements H_{ij}^{2h}. In all our calculations presented below, matrix elements Q_{ij} and H_{ij} are calculated using formulas (8).

To study the convergence of potential curves $E_i(\mathcal{R})$ and radial matrix elements $Q_{ij}(\mathcal{R})$ and $H_{ij}(\mathcal{R})$, we have performed a set of computations of these quantities as functions of the numerical scheme parameters, namely, the number of isoparametric Lagrange elements $N_{\rm el}$, their order $N_{\rm pol}$, and the maximum number of terms $l_{\max}$ in the angular basis set expansion in l (see Eq. (9)). In the present work, the desired accuracy of the ground-state energy of He and H^- is set to 10^{-6} a.u. This requires the same accuracy of radial matrix elements. From the results of numerical experiments, the following set of numerical parameters has been chosen for the He $^1S^e$ state: $N_{\rm el} = 210$ (1471 grid points with $h = 0.00053$), $N_{\rm pol} = 7$, and $l_{\max} = 11$ (12 equations in Eq. (11)). The grid in $\mathcal{R}$ has been chosen as follows: 0.02(0.02)0.32(0.01)1(0.02)3(0.05)5(0.08)9(0.1)20(0.2)30(0.25)50 (number in parentheses denotes the step in $\mathcal{R}$). A banded system of 17,652 linear algebraic equations (Eq. (12)) has been solved with relative error tolerance $\epsilon = 10^{-10}$ at each value of hyperradius $\mathcal{R}$ with the mean half bandwidth $M = 54$ (maximum 96). In Fig. 1 we show the He $^1S^e$ potential curves $E_i(\mathcal{R})$, $i = 1, \ldots, 28$, correlating with the $n = 1$–$n = 7$ hydrogen-like states of He^+ as a function of the hyperradius $\mathcal{R}$. Clearly seen are points of avoided crossings [2, 6] where the radial nonadiabatic coupling terms are known [2, 6, 7] to peak. Such peaks are

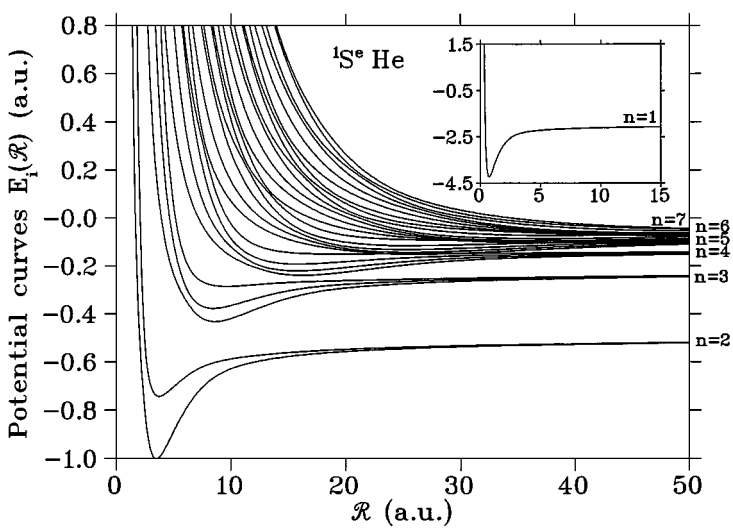

FIG. 1. Potential curves $E_i(\mathcal{R})$ (in a.u.) plotted vs hyperradius $\mathcal{R}$ up to the $n = 7$ threshold, $E_n = -2/n^2$, for the $^1S^e$ state of He.

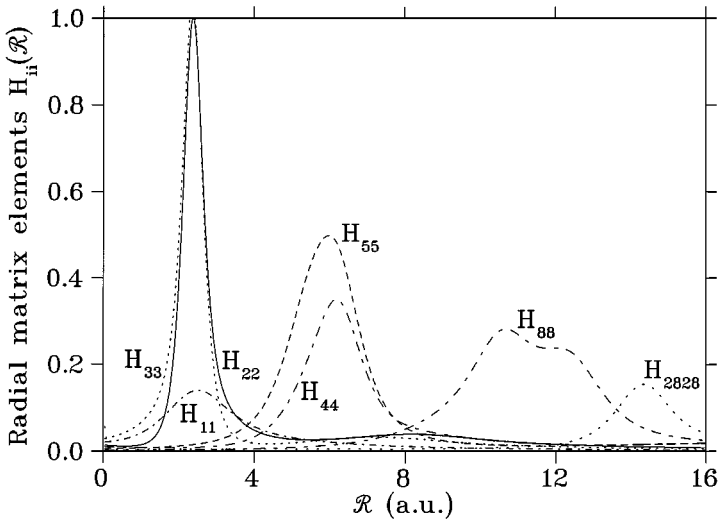

FIG. 2. Radial matrix elements $H_{ii}(\mathcal{R})$ for the $^1S^e$ state of He for $i = 1, 2, 3, 4, 5, 8$, and 28.

clearly seen from Fig. 2, where the diagonal matrix elements H_{ii}, $i = 1, 2, 3, 4, 5, 8, 28$, are presented. For instance, matrix elements H_{22} and H_{33} and also H_{44} and H_{55} in Fig. 2 show pronounced maxima in the avoided crossing regions.

In Fig. 3 we plot radial coupling matrix elements $Q_{ij}(\mathcal{R})$ for some values of i and j as functions of hyperradius $\mathcal{R}$. As seen in the figure, the matrix elements displayed also show maxima in the quasi-crossings points. Note that singular behavior of the radial matrix elements near avoided crossings can be eliminated by passing into the diabatic representation [25]. However, in this work we use the finite-element scheme which allows us to solve the eigenvalue problem for system of radial eauations (6) within the adiabatic representation.

In Table VIII we compare potential curves $E_i(\mathcal{R})$ calculated numerically with the asymptotic ones, $E_i^{\rm as}(\mathcal{R})$, computed analytically using the dipole approximation [26] for three

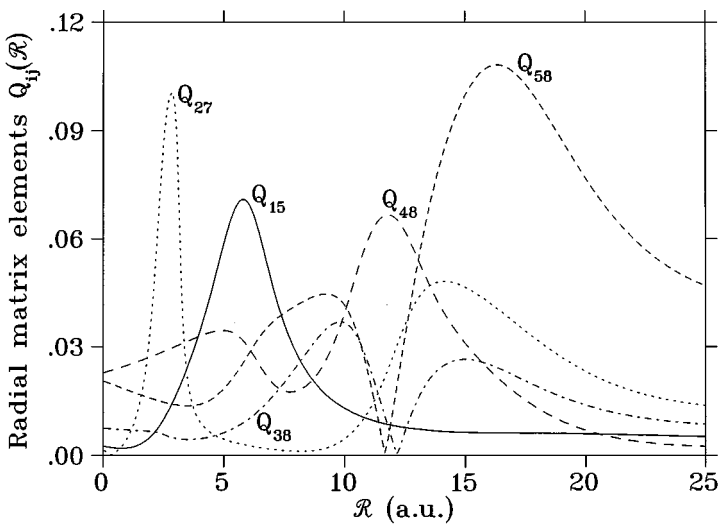

FIG. 3. Radial matrix elements $Q_{ij}(\mathcal{R})$ for the $^1S^e$ state of He for several values of i and j.

TABLE VIII

Comparison of the Numerical Potential Curves $E_i(\mathcal{R})$ with the Dipole Asymptotics, $E_i^{as}(\mathcal{R})$, for the $^1S^e$ State of He Calculated at $\mathcal{R}$ = 40, 60, and 80 a.u. up to the n = 3 Threshold

Curve number, i	$\mathcal{R} = 40$ a.u.		$\mathcal{R} = 60$ a.u.		$\mathcal{R} = 80$ a.u.	
	$-E_i(\mathcal{R})$	$-E_i^{as}(\mathcal{R})$	$-E_i(\mathcal{R})$	$-E_i^{as}(\mathcal{R})$	$-E_i(\mathcal{R})$	$-E_i^{as}(\mathcal{R})$
1	2.02516	2.02516	2.01674	2.01674	2.01254	2.01254
2	0.52627	0.52620	0.51722	0.51720	0.51281	0.51280
3	0.52413	0.52411	0.51628	0.51627	0.51228	0.51228
4	0.25103	0.25073	0.24052	0.24045	0.23563	0.23560
5	0.24735	0.24693	0.23888	0.23876	0.23470	0.23465
6	0.24437	0.24447	0.23765	0.23766	0.23403	0.23403

values of $\mathcal{R}$, 40, 60, and 80 a.u., up to the $n = 3$ threshold. It is evident that these results agree very well. For instance, the five significant digits are obtained for the ground-state potential curve ($i = 1$). This confirms the high accuracy of our numerical procedure.

For negative hydrogen ion H^- the following set of numerical scheme parameters has been chosen: $N_{el} = 220$ (1541 grid points with $h = 0.00051$), $N_{pol} = 7$, $l_{max} = 11$, and $\epsilon = 10^{-10}$. The hyperradius $\mathcal{R}$-region has been divided as follows: 0.02(0.08)0.98(0.02)1(0.025)3(0.05)5(0.075)7.1(0.1)20(0.2)30(0.25)50. The size of a banded system of linear algebraic equations (Eq. (12)) was 18,492 with the mean half bandwidth $M = 54$ (maximum 99). In Fig. 4 the H^- $^1S^e$ potential curves $E_i(\mathcal{R})$, $i = 1, \ldots, 28$, up to the $n = 7$ hydrogenic threshold are shown as functions of hyperradius $\mathcal{R}$. From the figure, one can see many quasi-crossing points, as well as several exact crossings.

As a useful check of the method, we have performed a number of bound-state calculations for He and H^-. Since our goal is to develop an efficient and stable algorithm for computing

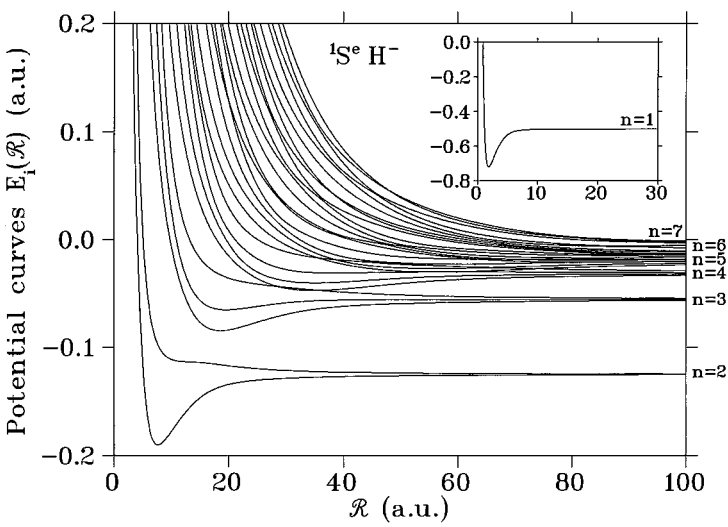

FIG. 4. Potential curves $E_i(\mathcal{R})$ (in a.u.) plotted vs hyperradius $\mathcal{R}$ up to the $n = 7$ threshold, $E_n = -1/2n^2$, for the $^1S^e$ state of H^-.

radial matrix elements that can be used in both scattering and bound-state calculations, we did not attempt to exceed the accuracy of the most accurate *ab initio* methods by pushing the bound-state calculation to complete convergence. Below we present the results of the ground-state energy calculation for He and H^-. The accuracy of the ground-state energies obtained is analyzed and compared with the accuracy of approximations made during the computation of the relevant matrix elements of radial coupling.

The system of coupled radial equations (6) has been solved, subject to boundary conditions (7), by the finite-element method using schemes of high-order accuracy [19, 20]. Isoparametric Lagrange elements of the third order have been used, providing an accuracy of order $O(h_{\mathcal{R}}^6)$ with respect to eigenvalues and of $O(h_{\mathcal{R}}^6)$ order with respect to eigenfunctions. Here $h_{\mathcal{R}}$ is the maximum mesh step of the finite-element grid on the interval $[0, \mathcal{R}_{\max}]$. As a result of numerical experiments, the following values of numerical scheme parameters have been chosen: (i) $\mathcal{R}_{\max} = 40$ a.u. and $N_{\rm el} = 1500$ (4501 grid points with step $h_{\mathcal{R}} = 0.0089$) for the He atom; and (ii) $\mathcal{R}_{\max} = 30$ a.u. and $N_{\rm el} = 1200$ (3601 grid points with $h_{\mathcal{R}} = 0.0082$) for the H^- ion. The size of a banded system of linear algebraic equations (Eq. (12)) that approximated a system of 28 radial equations was 125,972 with $M = 70$ (maximum 112) for the He and 100,772 with $M = 70$ (maximum 112) for the H^-, respectively. Error tolerance has been set to 10^{-12} a.u.

A study of the convergence of the ground-state energy of He and H^- with the number of radial equations is presented in Table IX. One can see that the energy eigenvalues converge monotonically from above, with the 28-channel value being $E_{\rm He} = -2.90372266$ a.u. and $E_{\rm H^-} = -0.52774970$ a.u. As shown in Table X, these values are close to the precision variational results: $E_{\rm He}^{\rm VAR} = -2.9037243770341195938$ a.u. [29] and $E_{\rm H^-}^{\rm VAR} = -0.527751016544306$ a.u. [30]. Since the calculation accuracy for eigenvalues equals $O(h_{\mathcal{R}}^6)$ and the basis step of the grid amounts to ≈ 0.009, our results have errors in the 12th digit. However, as follows from Table X, our energy values lie above the variational energies by approximately 10^{-6} a.u. This is consistent with the accuracy of the radial matrix elements and the approximations used. Comparisons with some other calculations are also given in Table X. It is evident that our results are more accurate than the 17-channel hyperspherical artificial channel method [23] and the hyperspherical close-coupling method [27, 28]. Both of these methods use the sector-diabatic representation, in which adiabatic basis expansion has a slower convergence than in the adiabatic representation used in the present work. We also

TABLE IX

Convergence of the Ground-State Energy (in a.u.) for He and H^- with the Number of Coupled Channels *n*

n	He	H^-
1	−2.88791168	−0.52241442
2	−2.89137991	−0.52472087
3	−2.90287002	−0.52732522
6	−2.90300448	−0.52751473
10	−2.90363613	−0.52768020
15	−2.90370549	−0.52773607
21	−2.90372264	−0.52774928
28	−2.90372266	−0.52774970

TABLE X
Comparison of the Present Ground-State Engergy (in a.u.) of He and H^- with Other Theoretical Calculations

Method	He	H^-
HACC[a]	−2.903723	−0.527750
ACM[b]	−2.903611	−0.527642
HSCC[c]	−2.903594	−0.52773
VAR[d]	−2.903724	−0.527751
MCHF[e]	−2.902909	−0.527542
CI[f]	−2.903724	−0.527542
RMM[g]	−2.8961	−0.52403
CCM[h]	−2.8934	−0.52775

[a] Present 28-channel hyperspherical adiabatic coupled-channel calculation.

[b] 17-channel hyperspherical artificial channel method calculation [23].

[c] Hyperspherical close-coupling calculation: 28-channel computation for H^- [27] and 21-channel calculation for He [28].

[d] Variational method calculation: using uncoupled correlated basis of 8066 one-dimensional functions for He [29] and 616 Hylleraas-type functions for H^- [30].

[e] Multiconfigurational Hartree–Fock calculation: using 32 configurations for H^- [31] and 10 configurations for He [32].

[f] Configuration interaction method calculation: using 130 configurations for H^- [33] and 125 modified configurations for He [34].

[g] R-matrix method calculation: using 158 configurations for H^- [35] and 79 configurations for He [36].

[h] Close-coupling method calculation with pseudostates and correlation terms: nine Hylleraas-type functions for H^- [37] and seven correlation functions for He [38].

compare our calculations with the results of the multiconfigurational Hartree–Fock method [31, 32], the configuration interaction method [33, 34], the R-matrix method [35, 36], and the close-coupling method [37, 38]. All these methods use a large number of electronic configurations, as seen in Table X. Analysis of the table shows excellent agreement with the results of the most accurate *ab initio* methods widely used in atomic and molecular calculations.

8. CONCLUSIONS

In the present work, the quantum mechanical three-body problem with Coulomb interaction has been formulated within the adiabatic representation method using hyperspherical coordinates. The reduction of the three-dimensional problem to a one-dimensional one has been performed using the Kantorovich method. A new method for computing variable coefficients (potential matrix elements of radial coupling) of a final system of ordinary second-order differential equations has been proposed. In this method, a new boundary parametric problem with respect to unknown derivatives of eigensolutions in the adiabatic variable (hyperradius) has been formulated. An efficient, fast, and stable algorithm for solving the boundary problem with the same accuracy for the adiabatic eigenfunctions and their derivatives has been suggested. As a result, matrix elements of radial coupling can be

calculated with the same precision as the adiabatic functions obtained as solutions of an auxiliary parametric eigenvalue problem.

The method developed has been thoroughly tested on a parametric eigenvalue problem for a hydrogen atom on a three-dimensional sphere. This problem has an analytical solution, which allows direct comparison of our results with the exact solutions. Excellent agreement between the analytical and numerical results has been obtained. The accuracy, efficiency, and robustness of the algorithm have been studied for this problem in details. The method has been further applied to the computation of the ground-state energy of the helium atom and the negative hydrogen ion. The results obtained show excellent agreement with the results of calculations by other methods.

This study constitutes a major improvement over the standard techniques for the calculation of potential matrix elements of radial coupling within the adiabatic representation method. It guarantees high accuracy of computation of radial matrix elements, comparable to the accuracy that can be achieved for the adiabatic eigensolutions of the auxiliary parametric eigenproblem. The method can be used not only for bound-state problems but also for solving, within the hyperspherical close-coupling approach, various scattering and photoionization problems arising in two-electron atomic systems. The approach proposed can easily be extended to systems with arbitrary (finite) masses of particles and total angular momentum $J > 0$, for any appropriate system of coordinates. The method can be also used for atom–diatom reactive scattering and photodissociation. Work on spectral characteristics and properties of exotic atoms within the present approach is currently under way [39].

ACKNOWLEDGMENTS

The authors express their gratitude to the seminar on Computational Physics of the Laboratory of Computing Techniques and Automation of the JINR and to Professor I. V. Puzynin for support of and interest in the work. This work was supported in part by JINR Project 09-6-0996-93/99, by the RFBR-INTAS under Grant 95-0512, by the RFBR under Grants 96-02-17715, 00-01-00067, 00-02-16337, and 00-02-81023, and by a Grant of the President of the Bulgarian State Agency of Atomic Energy.

REFERENCES

1. H. F. Mott and H. S. Massey, *Theory of Atomic Collisions*, 3rd ed. (Oxford Univ. Press, London/New York, 1965).
2. U. Fano and R. T. Rau, *Atomic Collisions and Spectra* (Wiley, New York, 1986).
3. *Atomic spectroscopy and collisions using slow antiprotons*, 7 Oct. 97, CERN/SPSC 97-19, CERN/SPSC P-307 (1997); *CERN Courier* **38**, No. 8 (1998).
4. M. Charlton, Prospects for low energy antihydrogen and the ATHENA project, in *Talk at VIII Int. Conf. on Symmetry Methods in Physics, July 28–August 2, 1997* (Dubna, Russia, 1997); M. Charlton, *Yad. Fiz.* **61**, N. 11 (1998).
5. S. I. Vinitsky and L. I. Ponomarev, *Fiz. Elem. Chastits At. Yadra* **13**, 1336 (1982); S. I. Vinitsky and L. I. Ponomarev, *Sov. J. Part. Nucl.* **13**, 557 (1982); L. Bracci and G. Fiorentini, *Phys. Rep.* **86**, 169 (1982).
6. J. Maček, *J. Phys. B* **1** (1968) 831; U. Fano, *Rep. Prog. Phys.* **46** (1983) 97; C. D. Lin, *Adv. Ato. Mol. Phys.* **22** (1986) 77; C. D. Lin, *Phys. Rep.* **257**, 1 (1995).
7. A. G. Abrashkevich, M. S. Kaschiev, I. V. Puzynin, and S. I. Vinitsky, *Sov. J. Nucl. Phys.* **48**, 602 (1986).
8. L. V. Kantorovich and V. I. Krilov, *Approximate Methods of Higher Analysis* (Wiley, New York, 1964; Gostekhteorizdat, Moscow, 1952).
9. A. G. Abrashkevich, D. G. Abrashkevich, M. S. Kaschiev, V. Yu. Poida, I. V. Puzynin, and S. I. Vinitsky, *J. Phys. B* **22**, 3957 (1989); A. G. Abrashkevich, D. G. Abrashkevich, I. V. Puzynin, and S. I. Vinitsky, *J. Phys. B*

24, 1615 (1991); A. G. Abrashkevich, D. G. Abrashkevich, M. S. Kaschiev, I. V. Puzynin, and S. I. Vinitsky, *Phys. Rev. A* **45**, 5274 (1992).

10. J. Botero, *Phys. Rev. A* **35,** 36 (1987); J. Zhou and C. D. Lin, *J. Phys. B* **27**, 5065 (1994).
11. S. Hara and T. Ishihara, *Phys. Rev. A* **40**, 4232 (1989); N. Fukuda, T. Ishihara, and S. Hara, *Phys. Rev. A* **41**, 145 (1990).
12. S. I. Vinitsky, V. S. Melezhik, L. I. Ponomarev, I. V. Puzynin, T. P. Puzynina, L. N. Somov, and N. F. Truskova, *Zh. Eksp. Teor. Fiz.* **79**, 698 (1980); S. I. Vinitsky, V. S. Melezhik, L. I. Ponomarev, I. V. Puzynin, T. P. Puzynina, L. N. Somov, and N. F. Truskova, *Sov. Phys. JETP* **52**, 353 (1980); I. V. Puzynin and S. I. Vinitsky, *Muon Catal. Fusion* **3**, 307 (1988).
13. F. Mrugala and D. Secrest, *J. Chem. Phys.* **78**, 5954, 5960 (1983); F. Mrugala, *J. Comput. Phys.* **58**, 113 (1985).
14. J. C. Light and R. B. Walker, *J. Chem. Phys.* **65**, 4272 (1976); B. Lepetit, J. M. Launay, and M. LeDourneuf, *Chem. Phys.* **106**, 103 (1986); D. M. Hood and A. Kuppermannn, in *Theory of Chemical Reaction Dynamics* (Reidel, Boston, 1986), pp. 193.
15. J.-Z. Tang, S. Watanabe, and M. Matsuzawa, *Phys. Rev. A* **46**, 2437 (1992); A. Igarashi and N. Toshima, *Phys. Rev. A* **50**, 232 (1994); B. Zhou and C. D. Lin, *Phys. Rev. A* **51**, 1286 (1995).
16. L. M. Delves, *Nucl. Phys.* **9**, 391 (1959); L. M. Delves, *Nucl. Phys.* **20**, 275 (1960); F. T. Smith, *Phys. Rev.* **120**, 1058 (1960).
17. G. Strang and G. J. Fix, *An Analysis of the Finite Element Method* (Prentice Hall, Englewood Cliffs, NJ, 1973).
18. K. J. Bathe, *Finite Element Procedures in Engineering Analysis* (Prentice Hall, Englewood Cliffs, NJ, 1982).
19. A. G. Abrashkevich, D. G. Abrashkevich, M. S. Kaschiev, and I. V. Puzynin, *Comput. Phys. Commun.* **85**(10) 65 (1995).
20. A. G. Abrashkevich, D. G. Abrashkevich, M. S. Kaschiev, I. V. Puzynin, and S. I. Vinitsky, *HSEIGV—A Program for Computing Energy Levels and Radial Wave Functions in the Coupled-Channel Hyperspherical Adiabatic Approach* (JINR Communications No E11-97-335, Dubna, 1997), pp. 27.
21. A. A. Izmes'tev, *Sov. J. Nucl. Phys.* **52**, 1697 (1990).
22. S. I. Vinitsky, L. G. Mardoyan, G. S. Pogosyan, A. N. Sissakyan, and T. A. Strizh, *Sov. J. Nucl. Phys.* **56**, 61 (1993).
23. A. G. Abrashkevich and M. Shapiro, *Phys. Rev. A* **50**, 1205 (1994).
24. A. G. Abrashkevich, D. G. Abrashkevich, and M. Shapiro, *Comput. Phys. Commun.* **90**, 311 (1995).
25. F. T. Smith, *Phys. Rev.* **179**, 111 (1969).
26. M. B. Kadomtsev, S. I. Vinitsky, and F. R. Vukajlovich, *Phys. Rev. A* **36**, 4652 (1987); A. G. Abrashkevich, D. G. Abrashkevich, I. V. Puzynin, and S. I. Vinitsky, *J. Phys. B* **24**, 1615 (1991).
27. J.-Z. Tang, Y. Wakabayashi, M. Matsuzawa, S. Watanabe, and I. Shimamura, *Phys. Rev. A* **49** (1994) 1021.
28. J. Z. Tang, S. Watanabe, and M. Matsuzawa, *Phys. Rev. A* **46**, 2427 (1992).
29. S. P. Goldman, *Phys. Rev. A* **57**, R677 (1998).
30. G. W. F. Drake, *Nucl. Inst. Meth. Phys. Res. B* **31**, 7 (1988).
31. H. P. Saha, *Phys. Rev. A* **38**, 4546 (1988).
32. C. F. Fischer and M. Idress, *J. Phys. B* **23**, 679 (1990).
33. M. Cortés and F. Martín, *J. Phys. A* **48**, 1227 (1993).
34. S. P. Goldman, *Phys. Rev. A* **52**, 3718 (1995).
35. H. R. Sadeghpour, C. H. Greene, and M. Cavagnero, *Phys. Rev. A* **45**, 1587 (1992).
36. P. Hamacher and J. Hinze, *J. Phys. B* **22**, 3397 (1989).
37. A. W. Wishart, *J. Phys. B* **12**, 3511 (1979).
38. J. A. Fernley, K. T. Taylor, and M. J. Seaton, *J. Phys. B* **20**, 6457 (1987).
39. A. G. Abrashkevich, M. S. Kaschiev, and S. I. Vinitsky, work in progress.